DEMONSTRATION REPORT

Tensor Invariant Processing of Multistatic EMI Data for Target Classification

Classification Demonstration - East Fork Valley Range Complex Former Camp Hale, Colorado

ESTCP Project MR-201310

JUNE 2017

Thomas Bell
Leidos

Dean Keiswetter
Acorn SI

REPORT DOCUMENTATION PAGE

Form Approved
OMB No. 0704-0188

1. REPORT DATE *(DD-MM-YYYY)*	2. REPORT TYPE	3. DATES COVERED *(From - To)*
06-30-2017	ESTCP Demonstration Report	6/12/2013 - 6/11/2018

4. TITLE AND SUBTITLE
Tensor Invariant Processing of Multistatic EMI Data for Target Classification

Classification Demonstration - East Fork Valley Range Complex
Former Camp Hale, Colorado

5a. CONTRACT NUMBER W912HQ-13-C-0040
5b. GRANT NUMBER
5c. PROGRAM ELEMENT NUMBER

6. AUTHOR(S)
Dr. Thomas Bell

5d. PROJECT NUMBER MR-201310
5e. TASK NUMBER
5f. WORK UNIT NUMBER

7. PERFORMING ORGANIZATION NAME(S) AND ADDRESS(ES)
Leidos Corporation
4001 N Fairfax Drive, Suite 675
Arlington, VA 22203

8. PERFORMING ORGANIZATION REPORT NUMBER
MR-201310

9. SPONSORING / MONITORING AGENCY NAME(S) AND ADDRESS(ES)
Environmental Security Technology Certification Program, 4800 Mark Center Dr
Suite 17D08, Alexandria, VA 22350-3605

10. SPONSOR/MONITOR'S ACRONYM(S)
ESTCP

11. SPONSOR/MONITOR'S REPORT NUMBER(S)
MR-201310

12. DISTRIBUTION / AVAILABILITY STATEMENT

DISTRIBUTION STATEMENT A. Approved for public release: distribution unlimited.

13. SUPPLEMENTARY NOTES

14. ABSTRACT
The objective of this demonstration is to demonstrate the classification performance of the procedures developed in SERDP projects MR-1711, MR-1658, and MR-2100 using data collected by URS Group, Inc. (URS) with the man-portable transient EMI (TEM) array (nicknamed "TEMTADS") at Former Camp Hale, CO. Detection is based on applying the standard dipole inversion model as a filter over the entire survey site. Locations where the model fits the measured data well are target locations. Classification decisions are based on two parameters easily calculated from magnetic polarizabilities of unknown targets and targets of interest. The parameters are measures of the mismatch between the strength and the shape of the respective polarizability curves. This approach has been applied to cued data at other Live Site Demonstrations, but has been applied to dynamic survey data here.

15. SUBJECT TERMS
Tensor Invariant Processing, Multistatic EMI Data, Target Classification, Camp Hale,

16. SECURITY CLASSIFICATION OF: a. REPORT	b. ABSTRACT	c. THIS PAGE	17. LIMITATION OF ABSTRACT	18. NUMBER OF PAGES	19a. NAME OF RESPONSIBLE PERSON / 19b. TELEPHONE NUMBER *(include area code)*
UNCLASS	UNCLASS	UNCLASS	UNCLASS	29	Dr. Thomas Bell / 703-312-6288

Standard Form 298 (Rev. 8-98)
Prescribed by ANSI Std. Z39.18

Contents

Figures

Tables

Acronyms

EFV	East Fork Valley
EMI	Electromagnetic Induction
EOD	Explosive Ordnance Disposal
ESTCP	Environmental Security Technology Certification Program
FOM	Figure of Merit
GPS	Global Positioning System
HEAT	High Energy Anti Tank
IDA	Institute for Defense Analyses
IMU	Inertial Measurement Unit
ISO	Industry Standard Object (one of several standardized pipe sections)
IVS	Instrument Verification Strip
MTADS	Multisensor Towed Array Detection System
MR	Munitions Response
ROC	Receiver Operating Characteristic
Rx	Receive
SERDP	Strategic Environmental Research and Development Program
SNR	Signal to Noise Ratio
TCRA	Time Critical Removal Action
TEM	Transient Electromagnetic
TEMTADS	Transient Electromagnetic MTADS
Tx	Transmit
URS	URS Group, Inc.
USFS	United States Forest Service

1.0 INTRODUCTION

The objective of this project is to test and evaluate new procedures for target detection and classification in the context of the Environmental Security Technology Certification Program (ESTCP) Classification Pilot Program Live Site Demonstrations. The procedures were developed in Strategic Environmental Research and Development Program (SERDP) projects MR-1711, MR-1658, and MR-2100. Detection is based on applying the standard dipole inversion model as a filter over the entire survey site. Locations where the model fits the measured data well are target locations. Classification decisions are based on two parameters easily calculated from magnetic polarizabilities of unknown targets and targets of interest. The parameters are measures of the mismatch between the strength and the shape of the respective polarizability curves. This approach has been applied to cued data at other Live Site Demonstrations, but has been applied to dynamic survey data here.

1.1 BACKGROUND

The characterization and remediation activities conducted at Department of Defense sites contaminated with unexploded ordnance (UXO) using 1990's and early 21st century technology often yield unsatisfactory results and are too expensive. In part, this is due to the inability of that technology to distinguish between UXO and non-hazardous items. Field experience has shown that when using the old technology over 90% of objects excavated during the course of remediation can be non-hazardous clutter.

SERDP and ESTCP have developed and tested several purpose-built multi-axis electromagnetic induction (EMI) sensor array systems for classifying buried objects at munitions response sites. They have also invested in developing new processing procedures optimized for this new generation of EMI sensors. This demonstration serves to evaluate the performance of procedures developed in SERDP projects MR-1711, MR-1658, and MR-2100.

1.2 OBJECTIVE OF THE DEMONSTRATION

The objective of this demonstration is to demonstrate the classification performance of the procedures developed in SERDP projects MR-1711, MR-1658, and MR-2100 using data collected by URS Group, Inc. (URS) with the man-portable transient EMI (TEM) array (nicknamed "TEMTADS" [1]) at Former Camp Hale, CO [2].

1.3 REGULATORY DRIVERS

The ESTCP has assembled an Advisory Group to address the regulatory, programmatic and stakeholder acceptance issues associated with the implementation of classification in the MR process. Additional details can be found in their guide to implementing advanced classification on munitions response sites [3].

2.0 TECHNOLOGY

The data collection technology and approach are discussed in the URS Demonstration Plan [2]. URS used the man-portable TEMTADS array to collect survey mode data which was used to identify metallic anomalies within the study area. The survey data were analyzed to produce a list of anomalies considered to have the potential to be targets of interest (TOI). They then parked the array over each of these anomalies in turn and collected "cued" data to be used for target classification. For this demonstration we will process the dynamic survey data to both determine the location of possible metallic anomalies and then calculate the likelihood that the anomaly is actually due to a TOI.

The processing and analysis procedures to be demonstrated were developed in SERDP projects MR-1711, MR-1658, and MR-2100 for use with the advanced EMI arrays developed by SERDP and ESTCP for target detection and classification.

In the field, cued locations were selected by looking at signal amplitude peaks above some reasonable threshold. This simple detection approach has two disadvantages. First, it only looks at the monostatic sensor channels (T_z-R_z) which typically, but not always, peak at the target's location. Second, the amplitude threshold is usually selected to find a certain TOI down to a maximum depth; this amplitude threshold will also include many small bits of clutter located on the surface. Instead of signal amplitude, we will apply the dipole model based detection filter developed under SERDP project MR-1711 [4]. This detection filter uses all transmit/receive channels from an advanced EMI sensor. The filter output peaks at the target's location based on the data's fit to the dipole model. The filter can be set to respond weakly to shallow clutter.

Classification typically involves comparing principal axis polarizabilities calculated from EMI data collected over an unknown target with those of known TOI [3]. The classification algorithm used here exploits the fact that an object's polarizability is a product of two factors: the volume of the object and a tensor whose eigenvalues depend only on the shape and composition of the object. Confronted with an unknown target, we compare its apparent size and EMI "shape" with the sizes and shapes of TOI. Classification is based on thresholding a figure of merit (FOM) parameter that is a weighted sum of parameters quantifying the mismatches in the EMI size and shape of the target relative to the TOI. For multiple TOI, the FOM is minimized over the set of TOI. This basic algorithm can also be used in cluster analysis to identify unexpected munitions. In this case each target is compared against all others to find groups which have similar EMI size and shape.

2.1 TECHNOLOGY DESCRIPTION

2.1.1 TEMTADS EMI Sensors

The man-portable TEMTADS array used in the Camp Hale demonstration consists of four single-axis transmit (Tx) coils and four three-axis receive (Rx) cubes arranged in a 2x2 array of Tx/Rx pairs. The picture on the left in Figure 1 shows one of the large (35 cm square by 8 cm high) Tx coils and one of the 8 cm Rx cubes which fits inside the foam core of the Tx coil. The middle picture shows three of the Tx/Rx pairs set into the plastic array enclosure. The centers of the Tx/Rx pairs are spaced 40 cm apart. The picture on the right shows the assembled array with its GPS antenna. The array is mounted on a cart with the coils 20 cm above the ground.

Figure 1. Man-portable TEMTADS array used in the Camp Hale demonstration.

Currents through the Tx coils illuminate a target in the ground under the array with an alternating bipolar magnetic field (primary field), which excites eddy currents in the target. In dynamic survey mode, the four Tx coils are fired sequentially: front left, front right, rear right, and rear left. All four Rx cubes record during each Tx, resulting in a total of 48 T_i-R_j channels of data. Figure 2 shows the four Tx current waveforms over a complete block of data. Each coil fires three bipolar pulses over a period of 1/30th of a second. The on/off duration of these pulses is 2.77 milli-seconds. The Rx coils measure the decay of the secondary magnetic field from the eddy currents during the off intervals between the alternating pulses of positive and negative Tx current. The measured responses are averaged over the duration after inverting those from the negative current pulses. The total time to fire all four transmits is 0.133 seconds. Given a platform speed of 0.8 m/s, the sensor moves roughly 0.1 m over this cycle and 0.025 m between each Tx.

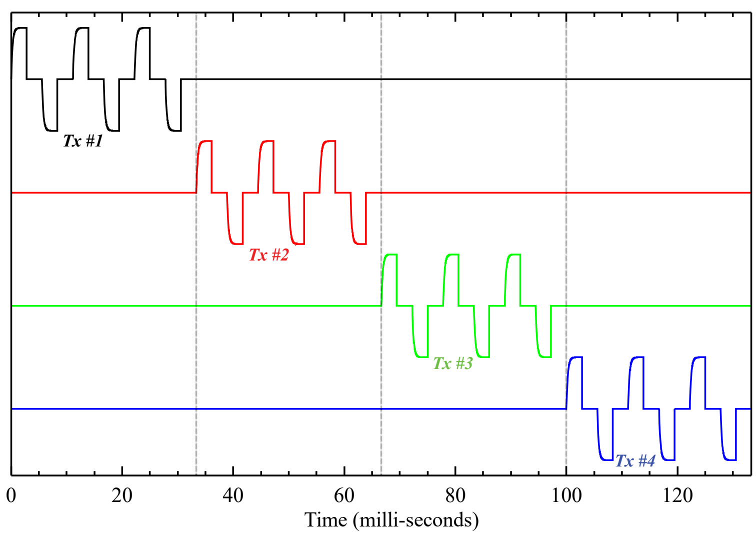

Figure 2. Dynamic TEMTADS transmitter current waveforms over one complete cycle.

Secondary field data are recorded for 19 time gates spaced logarithmically out to 2.77 milli-second after the primary field cutoff. Figure 3 is an example of the TEMTADS data collected as the platform moves over a target. Background response has been removed from the signals as described in section 2.1.2 below. Each panel corresponds to a different receive coil component, and different colors indicate which transmit coil is firing. The ordinate (vertical axis) scale is the background-subtracted signal in mV normalized by the peak Tx current and the abscissa (horizontal axis) scale is distance traveled. The data is for a single time gate at 0.137 milli-second after the transmit turn-off.

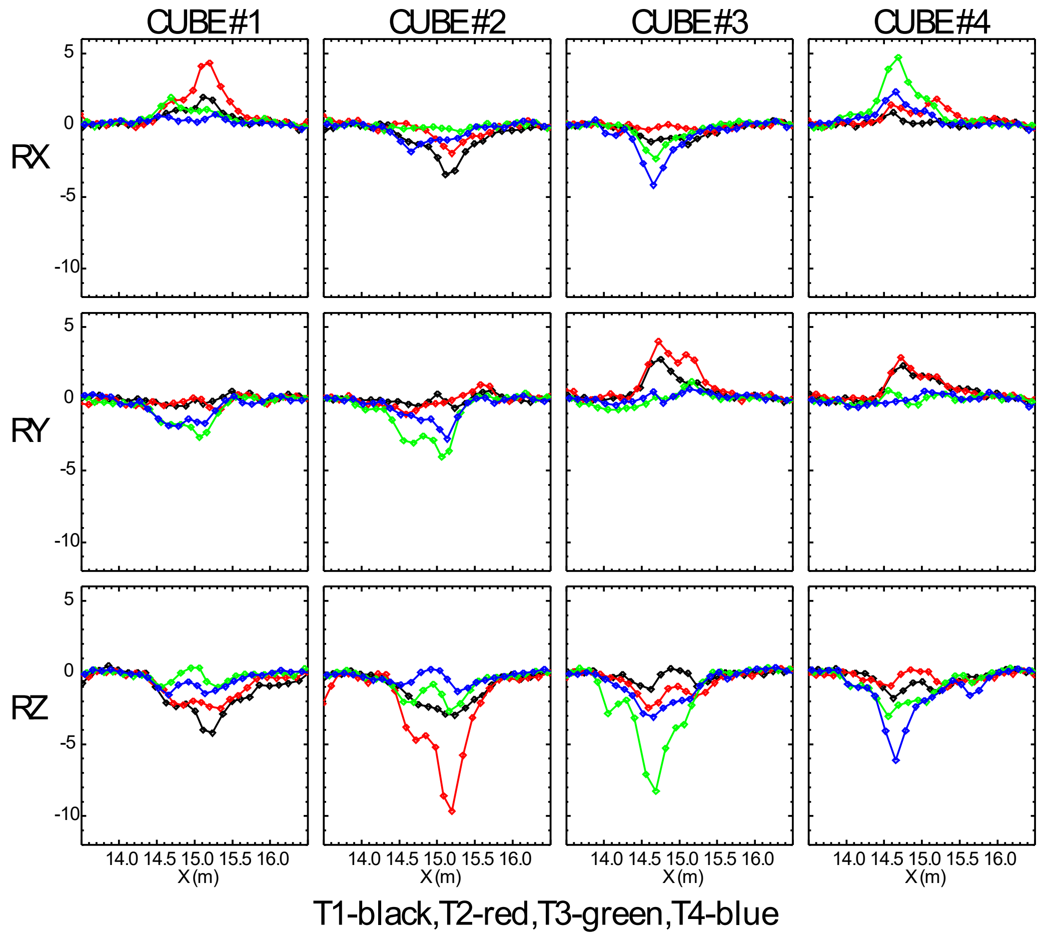

Figure 3. Sample TEMTADS dynamic data set. Ordinate is signal in mV normalized by Tx current, abscissa is distance traveled in meters. The plot colors indicate which transmit coil is firing.

2.1.2 Processing

Along with the EMI sensor data, one GPS record and one inertial measurement unit (IMU) record is collected for each complete transmit cycle. Each sensor has a different data rate, but the current TEMTADS system does not synchronize or adequately time stamp the positioning and EMI data. Current processing assumes the GPS positioning and IMU orientation occurs at the center of the transmit cycle. This results in position timing errors of up to one half of the transmit cycle, 0.133 seconds, or at a platform speed of 1.0 m/s, position errors up to 0.07 m. The orientation information from the IMU is used to map the GPS antenna position to the center of the EMI coils. A platform position and orientation is interpolated for each of the individual transmit coil firing times.

Bad sensor and poor positioning records are edited out. The EMI data are normalized by the peak transmit currents. Background levels are removed from the EMI data. For most of the data this is done by calculating a median level for the data file and subtracting it off. For data over dense target regions, a background region is manually selected and subtracted. Data collected over extremely dense target regions cannot be adequately zeroed.

All of the data files are merged for the entire site and the detection filter is run on this complete data set. Details of the filter can be found in the final report [4]. The filter output is on a regular grid across the site and ranges between 0 and 1 with larger values indicating target locations. Filter peaks are selected as possible target locations. Grid locations with little or no data present are flagged with a null value. These null regions can be flagged as missed. At each filter peak, a window of data is selected and an N-dipole inversion is run with N = 1, 2, 3 and 4. Each inversion results in target locations and polarizations. Repeated locations and bad polarization results are edited out. In moderately dense target regions, higher order N-dipole fits can be run. Extremely dense regions are processed to find TOI, but are flagged as areas where targets are probably being missed. This flagging is done manually based on large continuous areas where the measured signal amplitude and the detection filter output are significantly above the background (6 times RMS noise).

Compared to cued data, inversions from the dynamic data result in polarizations with fewer time gates (19 gates with 14 usable versus 120 with 110 usable) over a shorter decay duration (2.77 milli-seconds versus 25). The results are still be adequate for classifying targets and a similar process is applied. Because of increased sensor noise and platform positioning errors, there will be greater variability in the inverted polarizations which has to be accommodated in setting decision thresholds. Inversion results from previous dynamic survey sets and from the Camp Hale IVS strip assist in this process.

Figure 4 shows principal axis polarizabilities for two quite different objects: an ISO (left) and a piece of scrap metal (right) measured with the man-portable TEMTADS in dynamic mode at the Former Castner Range, TX. The objects are similar in size but have quite different shapes. Taken together the sets of three principal axis polarizabilities are quite different for the two objects.

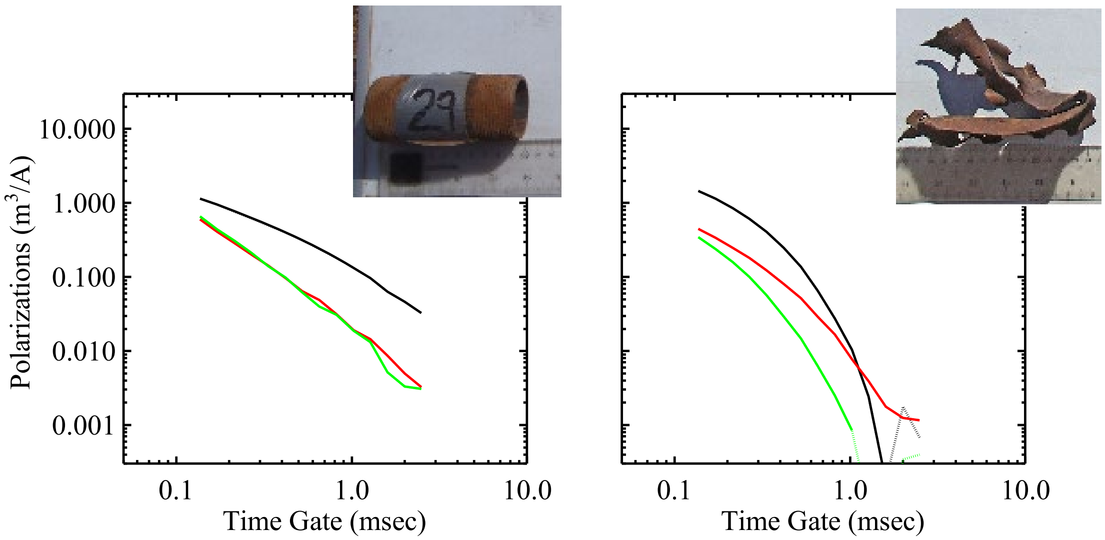

Figure 4. Principal axis polarizabilities for an ISO (left) and scrap metal (right). Polarizations inverted from dynamic data taken at Former Castner Range, TX.

Classification exploits these differences. Classification is a matter of deciding whether the object's polarizabilities are munitions-like or clutter-like. Library matching methods employing various procedures to compare polarizabilities of unknown targets with those of targets of interest (TOIs) are commonly used for classification. Ours exploits the fact that an object's polarizability tensor $\beta_{ij}(t) = V\alpha_{ij}(t)$ is a product of two factors: the volume V of the object and a tensor $\alpha_{ij}(t)$ whose eigenvalues $\alpha_j(t)$, i = 1, 2, 3 are determined by the shape and composition of the object. Confronted with an unknown target, we compare its apparent size and EMI "shape" with the sizes and shapes of the TOI.

Given the set (spanning three axes and N time gates) of principal axis polarizabilities β_0 for a TOI and the set of principal axis polarizabilities β for an unknown target, we calculate a size ratio s as

$$s = median\left(\frac{\sqrt[3]{\beta}}{\sqrt[3]{\beta_0}}\right)$$

where the median is taken over all axes and time gates for which the polarizabilities are above some threshold level which reflects the expected inversion noise. If a significant fraction (typically 25-50%) of the available polarizability terms are below this threshold, then the target is put in the "can't analyze" category.

The size mismatch parameter Δ_{size} is defined as

$$\Delta_{size} = \log(s)$$

which is equal to zero if the EMI sizes of the target and the reference TOI are the same. The shape mismatch parameter Δ_{shape} is determined by comparing the unknown target's polarizability with the reference polarizability scaled by the size mismatch

$$\Delta_{shape} = \frac{\sum\left|\sqrt[3]{\beta} - s\sqrt[3]{\beta_0}\right|}{\sum\sqrt[3]{\beta}}$$

in which the sums are over all terms with β above the noise level. For each target, size and shape mismatch parameters are calculated for each TOI. Classification is based on thresholding a figure of merit (FOM) parameter

$$FOM = \min_{TOI}\left\{|\Delta_{size}| + k\ log(\Delta_{shape})\right\}.$$

We have found that using a parameter value $k \approx 0.3$ gives the best classification performance. Low values of the TOI mismatch indicate a good match to both the size and the shape of the TOI. Minimizing the parameter over the set of TOI finds the best match to any TOI.

The TOI mismatch parameter typically runs between about -1 and 1, with TOI having the lowest values (best match of target polarizability strength and decay curve shapes to library polarizabilities) and clutter having the highest values (poor match to TOI polarizabilities). Figure 5 shows the distributions of the size and shape parameters (top plot) and the cumulative distribution of the net TOI mismatch (middle plot) for the man-portable TEMTADS array at the Camp Beale classification demonstration. Values for targets identified as TOI using the post-test ground truth are plotted in red and those for clutter items in blue.

Classification is based on thresholding a decision metric related to the TOI mismatch. For the sake of consistency with conventions used by other demonstrators (i.e., that TOI have large values of the decision metric and clutter items have small values) we define the decision metric as one over the antilog of the TOI mismatch, which works out to be

$$Decision\ Metric = \max_{TOI}\left\{\min\left(s, \frac{1}{s}\right)\left(\Delta_{shape}\right)^{-k}\right\}.$$

The first term in the curly brackets (s or s^{-1}, whichever is smaller) equals one when the EMI size of the target matches the TOI. Otherwise the value of the decision metric is reduced by the extent that the target size differs from the TOI size. The second term is larger when the polarizability shapes match well and smaller when they do not. The bottom plot in Figure 5 shows the decision metric values rank ordered from most like TOI to least like TOI. TOI values are shown in red and clutter values in blue. There is a distinct bend or slope break in the distribution as we go from TOI to clutter, followed by a gradual decline as we chew through the clutter items. We see similar patterns in the decision metric distributions obtained by re-processing data from other of the ESTCP Classification Pilot Program Live Site Demonstrations, leading us to conclude that with good quality control the stop-dig threshold may be set at the end of the slope break. As a practical matter the threshold has to be set low enough to capture those TOI which for some reason do not match the library specimens as well as most.

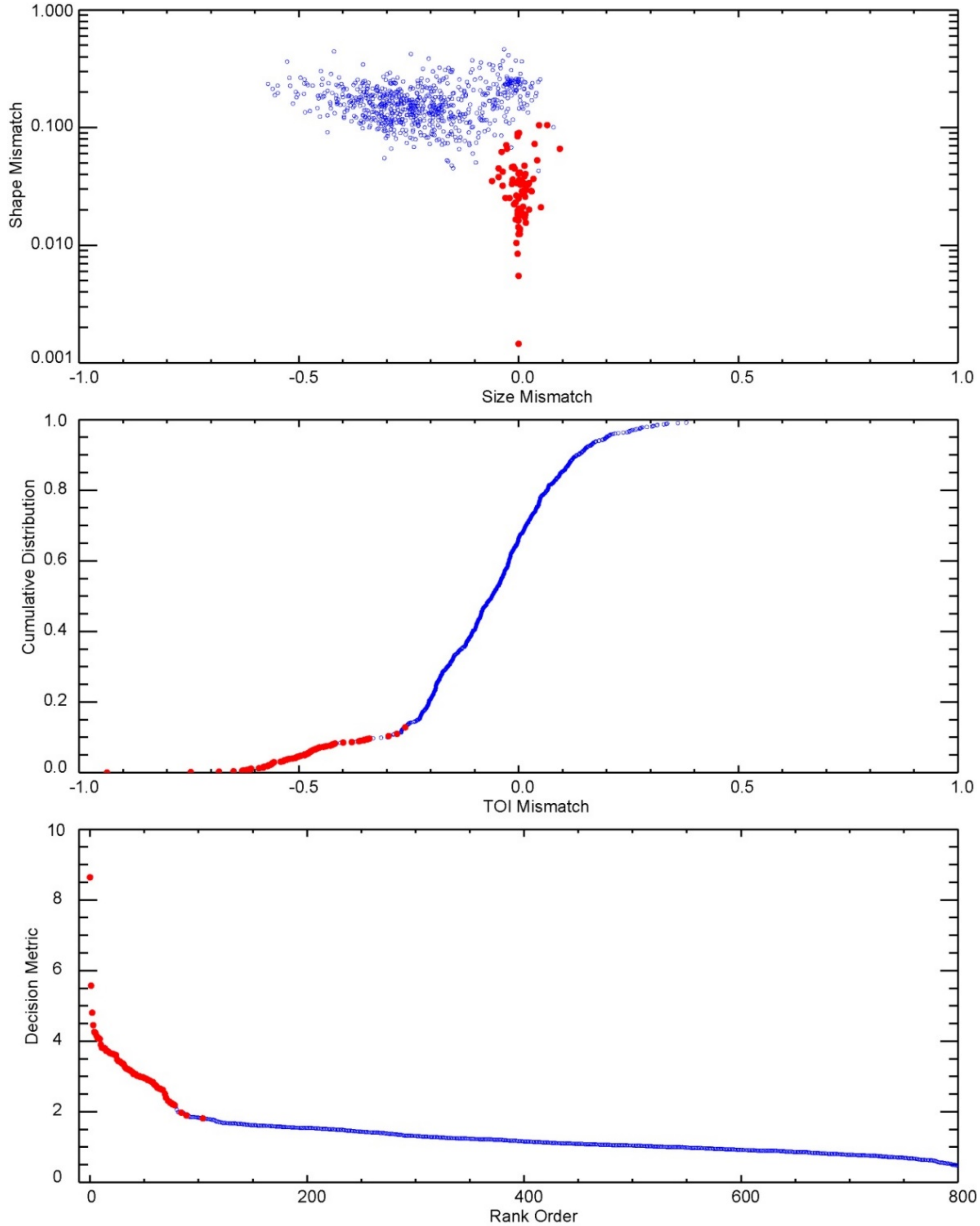

Figure 5. Classification parameter distributions for Camp Beale man-portable TEMTADS array demonstration. Top: scatter plot of size and shape mismatch parameters. Middle: cumulative distribution of net TOI mismatch figure of merit. Bottom: decision metric values rank ordered from most like TOI to least like TOI. Values for TOI items plotted in red, clutter items in blue.

2.2 ADVANTAGES AND LIMITATIONS OF THE TECHNOLOGY

The advantages of this technology are both quantitative and qualitative.

The detection filter improves upon the present signal amplitude approach [4]. It peaks at the target location. It can be set to reduce the response to surface clutter. A filter threshold can be set for a given TOI at desired depth based on the TOI's polarization and the actual measured survey noise.

For the classification approach, re-processing data from the recent Camp Beale demonstration produced a Receiver Operating Characteristic (ROC) which rises more rapidly and hits the 100% TOI recovered level with 50% fewer clutter digs beyond the training set than the ROC from conventional processing. Improved classification performance improves munitions response efficiency. The procedure operates in an intuitive and easily visualized feature space. It is transparent, objective and easily automated. All of this is likely to facilitate transition to production work and ease regulatory acceptance.

We anticipate no potential issues of concern or technical risks in taking the technology from the research phase to the proposed scale of the demonstration. This is a processing demonstration and we have re-processed and classified cued data from the recent Pole Mountain and Camp Beale demonstrations without incident. The detection filter has been tested on dynamic data from the Southwest Proving Ground and Castner Range demonstrations. No assumptions have been made that, if not realized, could impact the successful implementation of the project.

3.0 PERFORMANCE OBJECTIVES

The performance objectives for this demonstration are summarized in Table 2. The detection goal is to locate all TOI to within 0.4 m. The classification goal is to correctly identify all TOI as TOI and as many as possible clutter items as clutter. The fourth objective addresses how well we are able to specify the correct stop-dig threshold (i.e. which meets the classification objectives) in advance. The final two objectives refer to target feature extraction. As it turned out, only 372 out of several thousand detection locations we excavated, and IDA scoring reports were not produced. Our performance evaluation is based on a self-evaluation using the available ground truth. The results are in Sections 7.1 - 7.6.

Table 1. Performance Objectives

Objective	Metric	Data Required	Success Criteria
Maximize correct location of TOI	Distance of target locations from measured ground truth	• Ranked anomaly list • Scoring report from IDA	All target locations within 0.40 m of the ground truth
Maximize correct classification of TOI	Number of TOI retained	• Ranked anomaly list • Scoring report from IDA	Correctly classify all TOI
Maximize correct classification of clutter	Number of clutter digs eliminated	• Ranked anomaly list • Scoring report from IDA	Reduction of clutter digs by >85% while retaining all TOI
Specification of stop-dig threshold	Probability of correct TOI classification and number of clutter digs at threshold	• Stop-dig threshold • Scoring report from IDA	Stop-dig threshold to achieve classification objectives
Minimize number of anomalies that cannot be analyzed	Number of anomalies classified as "Can't Analyze"	Target parameters extracted from data collected over target	Reliable target parameters estimated for >95% of anomalies
Correct estimation of target parameters	Accuracy of estimated target parameters for seed items	Target parameters extracted from data collected over seeds	• Size mismatch within ±0.10 • Shape mismatch <0.2

4.0 SITE DESCRIPTION

The East Fork Valley (EFV) Range Complex within the Former Camp Hale, Colorado and is located on 382 acres in the White River National Forest approximately 10 miles south of Red Cliff and 18 miles north of Leadville off U.S. Highway 24. Eagle Valley was the primary area of Camp Hale first used by the Army for weapons training and later used by the Central Intelligence Agency. Currently, the United States Forest Service (USFS) manages the EFV. The EFV Range Complex is part of the National Historic Site, and USFS operates two active campgrounds (East Fork Group Campground and Camp Hale Memorial Campground) as well as other camp sites and trailheads which are regularly used along the banks of the East Fork of the Eagle River. Much of this range complex is accessible by the public with heavy recreational use. This ESTCP Live Site Demonstration will be conducted in a phased approach on no more than 25 acres within the EFV Range Complex. Site maps and additional relevant information are included in the URS Demonstration Plan [2]. The information in this section has been extracted from that report.

The specific types of conventional munitions used at Camp Hale were:

- Small arms: .22-, .30-, .45-, and .50-caliber ammunition;
- Demolition and bulk explosives;
- Hand Grenades: practice, smoke, and fragmentation;
- Rifle Grenades: practice, smoke, and high explosive anti tank (HEAT);
- Landmines: - Mine, Anti-Tank, Practice, M1;
  - Mine, Anti-Tank, HE, M1A1;
  - Mine, Anti-Tank, M4;
- Rockets: - 2.36-inch rockets (bazooka) – practice, smoke, and HEAT;
  - 3.5-inch rocket (bazooka) – practice, smoke, and HEAT;
  - 3.25-inch anti-aircraft target rockets;
  - 2.75-inch aircraft rockets;
- Mortars: 60mm, 81mm, and 4.2-inch – practice, illumination, and HE; and
- Projectiles: 37mm, 40mm, 57mm, 75mm, 76mm, 90mm, 105mm, 106mm, and 155mm

Two Time Critical Removal Actions (TCRAs) were performed in portions of the EFV in 2001 and 2003 to remove surface munition hazards in the valley floor. The following munitions types were found: 106mm HEAT recoilless rifles, 76mm recoilless rifle cartridges, 105mm discarding sabots, 57mm HEAT recoilless rifles, fragmentation hand grenades, WP smoke hand grenades, M9A1 rifle grenades (HEAT, Smoke, and Practice), 3.5-inch Bazooka HEAT rockets, 2.36-inch Bazooka HEAT rockets, 60mm mortar projectiles, 81mm mortar projectiles, 37mm artillery projectiles, 75mm artillery projectile, M1 anti-tank landmines, and live raw HE. During the TCRAs, 26 live HE items were found and 2 items were destroyed by Fort Carson Explosive Ordnance Disposal (EOD) personnel. Intact rifle grenades have been found at the Pistol Range and Machine Gun Range #4, indicating those areas have also been used as a rifle grenade ranges. Fort Carson EOD was notified; the rifle grenades were destroyed on site. Other live items have been discovered and disposed in the EFV area before the TCRAs including multiple intact rifle grenades and an 81mm mortar.

5.0 TEST DESIGN

5.1 BASIC EXPERIMENTAL DESIGN

The basic experimental design is described in the URS Demonstration Plan [2]. URS used the man-portable TEMTADS array to collect survey mode data which was used to identify metallic anomalies within the study area. The survey data were analyzed to produce a list of anomalies considered to have the potential to be targets of TOI. They then parked the array over each of these anomalies in turn and collected "cued" data to be used for target classification. We processed the dynamic survey data to both determine the location of possible metallic anomalies and then calculate the likelihood that the anomaly is actually due to a TOI. The processing and analysis procedures were developed in SERDP projects MR-1711, MR-1658, and MR-2100.

In the field, URS selected cued locations by looking at signal amplitude peaks above some reasonable threshold. This simple detection approach has two disadvantages. First, it only looks at the monostatic sensor channels (T_z-R_z) which typically, but not always, peak at the target's location. Second, the amplitude threshold is usually selected to find a certain TOI down to a maximum depth; this amplitude threshold will also include many small bits of clutter located on the surface. Instead of signal amplitude, we used the dipole model based detection filter developed under SERDP project MR-1711 [5]. This detection filter uses all transmit/receive channels from an advanced EMI sensor. The filter output peaks at the target's location based on the data's fit to the dipole model and is set to respond weakly to shallow clutter.

Classification involves comparing principal axis polarizabilities calculated from EMI data collected over an unknown target with those of known TOI [3]. The classification algorithm used here exploits the fact that an object's polarizability is a product of two factors: the volume of the object and a tensor whose eigenvalues depend only on the shape and composition of the object. Confronted with an unknown target, we compare its apparent size and EMI "shape" with the sizes and shapes of TOI. Classification is based on thresholding a figure of merit (FOM) parameter that is a weighted sum of parameters quantifying the mismatches in the EMI size and shape of the target relative to the TOI. For multiple TOI, the FOM is minimized over the set of TOI. This basic algorithm can also be used in cluster analysis to identify unexpected munitions. In this case each target is compared against all others to find groups which have similar EMI size and shape.

5.2 VALIDATION

The demonstration plan specified that at the conclusion of data collection activities, all anomalies on the master anomaly list assembled by the Program Office would be excavated. Validation was to be based on retrospective analysis using scoring results from the Institute for Defense Analysis (IDA). As it turned out, IDA scoring reports were not available so our results are based on a self-assessment using the available ground truth. Only a small set of the detected anomalies within the survey area were investigated intrusively: there were several thousand potential target locations but only 372 locations were excavated, yielding 632 items.

6.0 DATA ANALYSIS

The basic data analysis flow is:

1) Bad data (GPS or IMU problems) are dropped and remaining good survey data mapped.
2) The detection filter is run over the mapped data and filter peaks above threshold of 0.2 picked. The threshold of 0.2 corresponds roughly to a 37mm projectile at a depth of 0.30m.
3) At each detection filter peak N=1, 2 and 3 dipole fits are run on fixed windows of data.
4) The analyst picks spots to adjust the window and re-run fits with N=1, 2, 3, 4, 5, 6 dipoles. The adjustments accommodate bigger signal footprints, multiple overlapping footprints and indications of signal from a side object (e.g. corresponding to a large deep item dominated by small shallow one).
5) For each N-dipole fit spot, analyst identifies the most consistent fits.
    a. Consistent with Tz-Rz and detection filter footprint
    b. Consistent progression for N=1 to N=2, to N=3 …
    c. Physically sound polarization, non-negative, reasonable shape
6) For chosen fits, the analyst sets polarization weighting factors to emphasize non-negative, smooth decay shape, and suppress noisy results.
7) Scale/shape factors calculated using weights for 3 polarization, 2 polarization, 1 polarization, with a minimum of three gates needed.
8) Classification is based on the procedure described in Section 2.1.2.

7.0 PERFORMANCE ASSESSMENT

GPS was intermittently blocked by tree lines. Data with poor GPS was not used in our analysis. Nor was data with IMU errors or otherwise corrupted data. Areas with very high target density (edges of burn pits, etc.) and areas with poor coverage were also excluded. Table 2 shows the performance objectives from Section 3.0 along with the results. IDA scoring reports were not available so our results are based on a self-assessment using the available ground truth. The results are discussed in Sections 7.1 - 7.6 below.

7.1 DETECTION AND LOCATION OF TOI

The detection goal is to set a "flag" within 0.40 m of all items in the field. Only a small set of the detected anomalies within the survey area were investigated: there were several thousand potential target locations but only 372 locations were excavated, yielding 632 items. The locations for ground truth excavation were picked in the field based on signal amplitude and not the detect filter output. Matching detection filter targets to ground truth targets on a one-to-one basis was not feasible. For our analysis we simply matched detect filter targets to the closest ground truth locations.

Fifty-one of the ground truth locations were in areas of dense signal or poor coverage where we could not apply the detection filter. Twenty-two were in grids 13004 and 13005 where no

Table 2. Performance Assessment Results

Objective	Metric	Data Required	Success Criteria	Results
Maximize correct location of TOI	Distance of target locations from measured ground truth	• Ranked anomaly list • Ground truth	All target locations within 0.40 m of the ground truth	All TOI within 0.4 m
Maximize correct classification of TOI	Number of TOI retained	• Ranked anomaly list • Ground truth	Correctly classify all TOI	20 of 21 (95%) correctly classified
Maximize correct classification of clutter	Number of clutter digs eliminated	• Ranked anomaly list • Ground truth	Reduction of clutter digs by >85% while retaining all TOI	98% rejected while retaining all TOI in library
Specification of stop-dig threshold	Probability of correct TOI classification and number of clutter digs at threshold	• Stop-dig threshold • Ground truth	Stop-dig threshold to achieve classification objectives	Reduction of clutter digs by 83% while retaining all TOI in library
Minimize number of anomalies that cannot be analyzed	Number of anomalies classified as "Can't Analyze"	Target parameters extracted from data collected over target	Reliable target parameters estimated for >95% of anomalies	2-polarizability classification possible for 95% of anomalies
Correct estimation of target parameters	Accuracy of estimated target parameters for seed items	Target parameters extracted from data collected over seeds	• Size mismatch within ±0.10 • Shape mismatch <0.2	Size mismatch within ±0.10, shape mismatch <0.2

dynamic data was provided to us. Of the remaining 299 locations, 25 had no detect filter target within 0.60 m. Seventeen of these had weak signal amplitudes and detect filter response less than threshold. All were from small ignorable pieces of scrap metal. Three were listed as no contact in the ground truth. There was no signal or detect filter response at these locations. Two were on the edge of a larger signal object. Three more were on the edge of a poor coverage area.

Figure 6 shows the target location performance for the relevant 274 ground truth targets. For 265 of them (97%) the offset between the ground truth target location and a detection filter peak is less than 0.4 m (dashed circle). All of the 21 ground truth TOI in the areas where we had data were matched by potential target locations in the detect filter output in this central region.

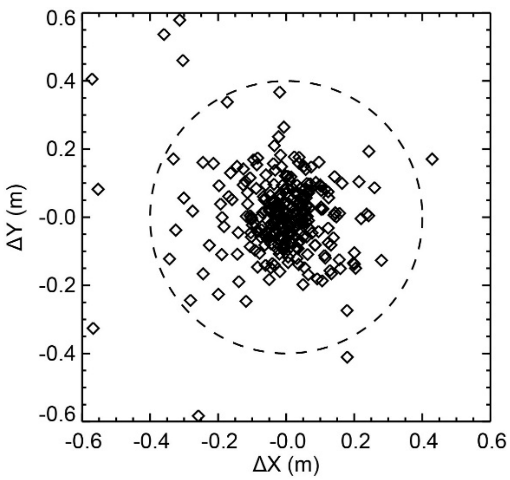

Figure 6. Target location performance: offsets between detection filter peaks and ground truth target locations.

7.2 CORRECT CLASSIFICATION OF TOI

Figure 7 shows the classification parameter distributions based on the MR-201424 Blossom Point library. (a) is a scatter plot of the size and shape mismatch parameters, (b) the cumulative distribution of the net TOI mismatch figure of merit and (c) the decision metric values rank ordered from most like TOI to least like TOI. Values for TOI items plotted in red.

There were 21 ground truth TOI in the areas where we had data: 17 Medium ISO's, two 81mm projectiles, one 60mm illumination round and one 40mm illumination round. All but the 40mm round (the red "outlier" in the plots) were correctly identified using the MR-201424 Blossom Point library. The library did not include a 40mm illumination round and it was missed by the library-based classification analysis. The principal axis polarizabilities extracted from the data for the missed 40mm round are shown in Figure 8. They are similar to those of fins and fuzes found at the site. This target corresponds to the uppermost red diamond in Figure 7(a). The polarizability strength matches up with the smaller targets in the library, so the size mismatch parameter is near zero. The round is basically a thin-walled aluminum cylinder. At early times the transverse polarizabilities are stronger than the axial polarizability, and at later times they all roll over into a rapid exponential decay. This behavior does not match up with any of the targets in the general library, and it has a much larger shape mismatch parameter than the other TOI. The failure was caused by several factors: ground truth for the entire site was not available and we could not get training data to possibly isolate the 40mm illumination round signature had there been enough others at the site, the 40mm illumination polarizabilities were similar to those many of the clutter items (fins, fuzes, etc.), and there were no other similar TOI in the library similar to the 40mm illumination round.

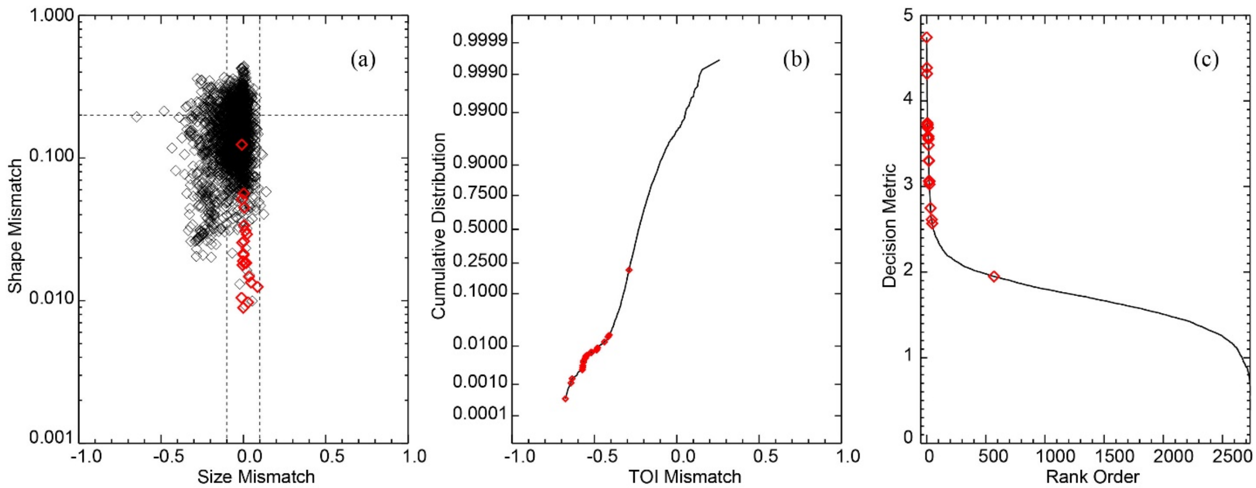

Figure 7. Classification parameter distributions using the MR-201424 library: (a) scatter plot of size and shape mismatch parameters. (b) cumulative distribution of net TOI mismatch figure of merit, (c) decision metric values rank ordered from most like TOI to least like TOI. Values for TOI items plotted in red.

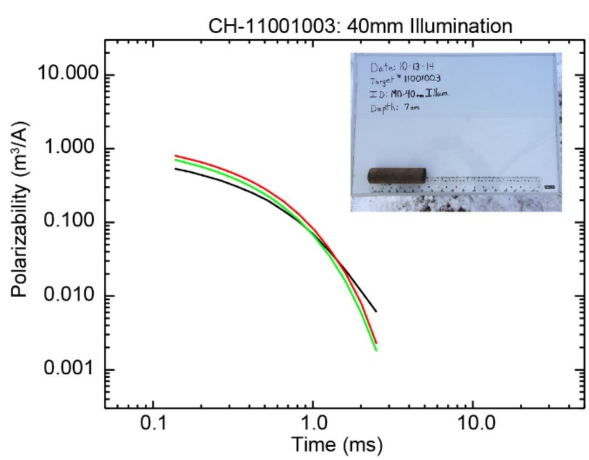

Figure 8. Target CH-11001003 (40mm illumination round) polarizabilities.

7.3 CORRECT CLASSIFICATION OF CLUTTER AND STOP DIG

All of the TOI in the MR-201424 library were correctly classified at a decision metric threshold of 2.5. At this level 2676 of 2734 possible clutter items (98%) were rejected. Using the "knee" of the decision metric curve (metric value 2.0), all of the TOI in the library (20 of 21 targets) are correctly identified as TOI and 2280 of the 2734 possible clutter items (83%) are rejected. With the missed item added to the library the knee of the decision metric curve is broader due to fins and fuzes which match fairly well to the 40mm illumination round. In this case 2060 of the 2734 possible clutter items are rejected (~75%).

7.4 CAN'T ANALYZE

We used a criterion of at least three good time gates to calculate shape/scale match to the library. To use all three polarizations in the match, 2734 of 3278 targets (83%) can be used. For a two-polarization match, 3119 of 3278 (95%) can be used. Most of remaining polarizations can be rejected on basic object size, i.e. polarizations are too small to be an object of interest.

7.5 TARGET PARAMETER ASSESSMENT

The dotted lines in Figure 7(a) show the success criteria. The size mismatch is within ±0.1 and the shape mismatch is <0.2 for all of the TOI using the MR-201424 Blossom Point library.

8.0 COST ASSESSMENT

Table 3 shows the cost elements tracked during the demonstration. This is a data processing and analysis demonstration. Data collection costs can be found in the URS demonstration report [6]. The costs in Table 3 are given in hours per task based on the number of days devoted to the task for the Dynamic Data Processing and Target Selection. Computer time for computationally intensive tasks (running the detection filter and multi-dipole fits) is not included. In those cases the processing was set up and run while the analyst was otherwise occupied (e.g. overnight).

The first item in the analysis chain (Dynamic Data Processing) is mapping of the survey data. Bad data (GPS, IMU or TEM data problems) are dropped and remaining good survey data mapped. There were significant problems with the data (IMU and TEM data dropouts, GPS loss, etc.) which took a significant amount of time to diagnose and fix or edit out. The next step (Target Selection) includes time required to run and evaluate detection filter and N-dipole target picks. The detection filter is run over the mapped data and filter peaks above threshold of 0.2 picked. The threshold of 0.2 corresponds roughly to a 37mm projectile at a depth of 0.30m. At each detection filter peak N=1, 2 and 3 dipole fits are run on fixed windows of data. This process was also labor intensive. Complex regions with high target density required significant amounts of time to evaluate. More open areas took very little time. Semi-automated procedures for dealing with data mapping and target selection problems should be integrated into UX-Analyze. In that event dynamic data processing and target selection costs should be significantly reduced, Once the data were mapped and targets selected, the next steps (Feature Extraction, Training and Classification were straightforward. Because of the limited ground truth, training data was not available and this step was restricted to running the MR-201424 library and subsets of the library. The analyst identified the most consistent fits consistent with the progression of N=1, 2, 3… dipole fits and calculated the scale/shape parameters for the library matches. Classification was based on the procedure described in Section 2.1.2

Table 3. Demonstration costs.

Cost Element	Data to be Tracked	Estimated Cost
Pre-demonstration development	Time required to re-process data from previous demonstrations and establish QA/QC procedures	Not tracked
Dynamic Data Processing	Time required to process raw dynamic survey data into workable, merged data set	90 hr
Selection of Targets	Time required to run and evaluate detection filter and N-dipole target picks	90 hr
Feature Extraction	Time required to calculate principal axis polarizabilities.	6 hr
Training	Time required to perform cluster analyses and establish appropriate TOI libraries	2 hr
Classification	Time required to apply classification algorithms and produce dig list.	1 hr

9.0 MANAGEMENT AND STAFFING

Table 4 presents key personnel and their responsibilities for this demonstration. Contact information for key personnel included as Appendix B.

Table 4. Key personnel and responsibilities.

Name	Title	Organization	Responsibilities
Herb Nelson	MR Program Manager	ESTCP	• Manage MR project for ESTCP
Victoria Kantsios	Project Manager	URS	• URS Project Manager • Serve as the single point of contact for management and technical direction of URS demonstration. • Coordinate daily work and ensure technical quality of project activities.
Cheryl Gannon	Project Geophysicist	URS Consultant	• URS Project Geophysicist • Serve as the primary point of contact for technical coordination of project geophysical requirements • Coordinate daily work and ensure technical quality of geophysical activities • Perform data processing and target selection • Provide raw and validated processed data to the Project Manager
Tom Bell	Principal Investigator	Leidos	• Principal Investigator • Serve as the primary point of contact for technical coordination of project requirements
Bruce Barrow	Analyst	Leidos	• Perform dynamic data analysis and classification

10.0REFERENCES

1. James B. Kingdon, Bruce J. Barrow, Thomas H. Bell, David C. George, Glenn R. Harbaugh and Daniel A. Steinhurst, "TEMTADS Adjunct Sensor Systems: Hand-held EMI Sensor for Cued UXO Discrimination (ESTCP MR-200807) and Man-Portable EMI Array for UXO Detection and Discrimination (ESTCP MR-200909) Final Report," Naval Research Laboratory Memorandum Report NRL/MR/6110--12-9401, April 5, 2012.

2. ESTCP project MR-201230 Demonstration Plan, "Demonstration of Advanced Geophysics and Classification Methods on Munitions Response Sites - East Fork Valley Range Complex, Former Camp Hale, Colorado," August 2014.

3. Anne Andrews and Herb Nelson, "Implementing Advanced Classification on Munitions Response Sites: A Guide to Informed Decision Making For Project Managers, Regulators, and Contractors," ESTCP Final Report, December 2011.

4. Thomas H. Bell and Bruce Barrow, “Bulk Magnetization Effects in EMI-Based Classification and Discrimination,” SERDP Project MR-1711 Final Report, March 2015.

5. Thomas H. Bell and Bruce Barrow, “Bulk Magnetization Effects in EMI-Based Classification and Discrimination,” SERDP Project MR-1711 Final Report, March 2015.

6. V. Kantsios, C. Gannon and B. Helmlinger, “Demonstration of Advanced Geophysics and Classification Methods on Munitions Response Sites: East Fork Valley Range Complex Former Camp Hale, CO,” ESTCP Project MR-201230 Technical Report, April 2016.

APPENDIX A. HEALTH AND SAFETY PLAN

The Health and Safety Plan for the on-site activities at Camp Hale is included in the URS Demonstration Plan [2].

APPENDIX B. POINTS OF CONTACT

Point of Contact (Organization)	Mailing Address	Phone and e-mail	Role in Project
Herb Nelson (ESTCP)	4800 Mark Center Drive, Suite 17D08 Alexandria, VA 22350	Office: 571-372-6400 herb.nelson@nrl.navy.mil	MR Program Manager
Victoria Kantsios (URS)	2450 Crystal Drive, Suite 500 Arlington, VA 22202	Office: 703-418-3030 Cell: 404-702-1141 victoria.kantsios@urs.com	URS Project Manager
Heesoo Chung (URS Consultant)	24164 E 4th Drive Aurora, CO 80018	Office: 303-868-9309 Impulse04@gmail.com	URS Project Geophysicist
Tom Bell (Leidos)	4001 N. Fairfax Dr., Suite 7132 Arlington, VA 22203	Office: (703) 312-6288 Cell: (301) 712-7021 bellth@leidos.com	Principal Investigator